NEW IMPLEMENTATION OF THE CONJUGATE GRADIENT BASED ON THE IMPEDANCE OPERATOR TO ANALYSE ELECTROMAGNETIC SCATTERING

H. Belhadj and S. Mili

SysCom laboratory, National Engineering School of Tunis
B. P. 37, Le Belvedere 1002, Tunis, Tunisia

T. Aguili

SysCom Laboratory
National Engineering School of Tunis, Tunisia

Abstract—An original iterative method based on the conjugate gradient algorithm is developed in this paper to study electromagnetic scattering. The Generalized Equivalent Circuit (GEC) method is used to model the problem and then deduce an electromagnetic equation based on the impedance operator. For validation purposes, the developed method has been applied to various iris structures. Results computed using the new implementation of the conjugate gradient are similar to theoretical values. The field and current distribution are identical to the ones obtained with the moment method. Moreover, the memory resources required for storage are significantly reduced.

1. INTRODUCTION

The study of electromagnetic wave scattering has known considerable theoretical progress [1]. Numerical methods such as the finite element method [2], the moment method [3, 4]... etc. were used to study the electromagnetic wave scattering of any given structure. However, when such methods are applied to large structures, important storage resources and processing time are required limiting then their range of applicability. To circumvent these limitations, iterative approaches have been investigated. Among these approaches, we are interested to

the conjugate gradient (CG) method [5, 6]. This method is a finite step iterative method which converges to the solution for any initial guess.

Due to its efficiency, variants of this method have been exploited to study electromagnetic problems [6–12]. It has received widespread use in electromagnetic domain with the works of Sarkar, Arvas and Rao [9], Barkeshli and Volakis [11], when they have combined the CG algorithm with the fast Fourier Transform (FFT) technique. This method called "CGFFT" reduces computational time and computer storage compared to the ordinary CG method.

In this paper, a new formulation of the CG method has been developed to study the electromagnetic scattering. The main idea is to combine the ordinary CG method to the Generalized Equivalent Circuit (GEC) modeling [13–16]. In this formulation, the impedance operator is used instead of the integro-differential operator [9] simplifying then the transition between spectral and spatial domains.

The developed method has been applied to solve electromagnetic equation for some post and iris structures located in the cross section of a rectangular waveguide.

This paper is organized as follows: Section 2 presents the studied structures and the problem formulation; it describes the methodology to extract the equivalent circuit and explains how the Method of Generalized Equivalent Circuit (GEC) is used to identify the equation based on the impedance operator. It also reminds the conjugate gradient algorithm principle and its application to solve the operator equation obtained. The sections which follow deal with numerical results: the current obtained has been represented for some post and iris structures, and the electric field resulted has been compared to the one computed by the MoM.

2. PROBLEM FORMULATION

As an example of a scattering problem to be solved using the new formulation of CG, let us consider the scattering from a post and from an iris located in an infinite rectangular waveguide as shown in Figures 1(a) and 1(b). These structures are excited by the fundamental mode of the rectangular waveguide enclosing them.

We are using a uniform waveguide of rectangular cross section; a and b design respectively the cross section length and width, d is the window width in Figure 1(a) and the metal width in Figure 1(b). D is a symmetric plan for the structure; it designs the discontinuity plan on which we consider a magnetic wall.

Two types of waveguides are tested in this work. The first waveguide called EMEM waveguide is composed of two perfect electric
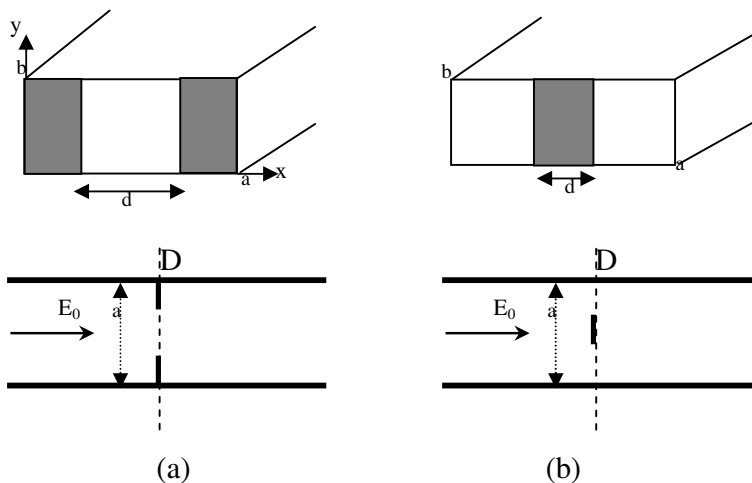
Figure 1. (a) Inductive iris, (b) inductive post.

walls to the top and the bottom, lateral walls are magnetic. The second type consists of four electric walls, it is noted EEEE waveguide. The considered waveguides are lossless.

2.1. Structure Modeling

The studied problem is modeled using the GEC method [13–16] which translates the boundary conditions and the relations between electric and magnetic fields into an equivalent circuit. In order to satisfy the boundary conditions we have introduced the Heaviside operators $\widehat{H}_i$ and $\widehat{H}_m$, which are respectively the indicator of the isolator part of the obstacle and the metallic part.

The discontinuity surface can be dissociated into a metallic surface and a dielectric surface. The virtual current source J is defined on the metallic surface and is null on the dielectric part. We note E its dual. This source behave as a short circuit on the metallic surface ($\widehat{H}_m E = 0$), and it is equivalent to an open circuit on the dielectric ($\widehat{H}_i J = 0$). This virtual current source is then representing all the boundaries conditions on the symmetric plan D of the structure.

Figure 2 represent the equivalent circuit of the structures given in Figure 1.

The real source E represents the fundamental mode in rectangular waveguide, and $\widehat{Z}$ is the impedance operator corresponding to evanescent modes.
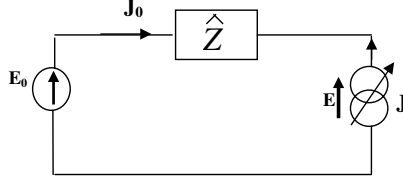
Figure 2. The equivalent circuit of the structure.

The boundary conditions of magnetic field are translated in this representation by the Kirchhoff law applied to the electric field [16]. This method allows us to identify the relation between the electric field and the current using the impedance operator. In fact, when we apply the laws of tension and current, we deduce the relation between virtual and real sources and its duals.

From this circuit, we can deduce the following system:

$$\begin{cases} J_0 = -J \\ E = E_0 + \widehat{Z}J \end{cases} \tag{1}$$

The first part of this system presents the continuity relation of the current on the discontinuity surface. Remind that J designs the current density of the source $(J_0 = \vec{H}_0 \wedge \vec{n})$ and J is the current density on the iris.

The second part of the system designs the continuity relation of the electric field at the iris/source discontinuity surface.

So the equation verified on the metallic part of the structure is given by:

$$\widehat{H}_m \widehat{Z} J = -\widehat{H}_m E_0 \tag{2}$$

We remind that the impedance operator is given by the following formal relation [16, 19]

$$\widehat{Z} = \sum_{n=1,2,3,\dots} |f_n\rangle z_n \langle f_n| \tag{3}$$

The operator $\widehat{Z}$ is, in fact, equivalent to the Green function on the spectral domain, decomposed on the considered mode basis of the structure. Particularly, it is the dyadic green function and in general, applied to a function ϕ it is given by: $\widehat{Z}\phi = \sum_n |f_n\rangle z_n \langle f_n | \phi\rangle$.

This represents the decomposition of a function ϕ on the modes basis f_n.

The scalar product $\langle u, v \rangle$ is defined on the Hilbert space, and is given by

$$\langle u , v \rangle = \int u^* v \quad u, v \in L^2 \tag{4}$$

where u^* designs the complex conjugate of u. z_n designs the impedance of each mode, and n is the mode number [17]

$$z_n = \frac{j\omega\mu_0}{\gamma} \tag{5}$$

where $\gamma = \sqrt{(\frac{n\pi}{a})^2 - k_0^2}$ denotes the propagation constant.

The f_n define the waveguide modal basis [17, 18] and are determined as a function of the waveguide type.

In the first case, the waveguide used is the EMEM guide. The fundamental mode is the transverse electromagnetic mode (TEM). We are interested to the study of scattering from the structure when excited by this fundamental mode.

The excitation (mode TEM) is independent of y. On the other hand, the discontinuity is uniform on the y-axis. As a consequence, studied problem has no y dependency. Also are the f_n modes excited by the scattering of the fundamental mode over the obstacle.

Due to the invariance of the problem, only TEM mode and Transverse Electric modes exist. The mode basis is then given as following:

$$\begin{cases} f_0 = E_0 = \frac{1}{\sqrt{a}} \\ f_n = \sqrt{\frac{2}{a}} \cos(\frac{n\pi}{a}x) \end{cases} \tag{6}$$

In the second case, the waveguide used is an electric one, so the excitation is the fundamental mode TE_{10}, and it is the only one propagating mode within the operating frequency band.

Due to the symmetry of the problem, the modal basis is independent of y. Then, the scattering of the fundamental mode over the structure excite only the TE modes which have the following expression:

$$\begin{cases} f_0 = E_0 = \sqrt{\frac{2}{a}} \sin(\frac{\pi}{a}x) \\ f_n = \sqrt{\frac{2}{a}} \sin(\frac{n\pi}{a}x) \end{cases} \tag{7}$$

In this paper, we focus on solving the given operator linear equation defined on the metallic part of the structure:

$$\widehat{Z}J = -E_0. \tag{8}$$

with $\widehat{Z}$ is an auto-adjoint operator, J and $E_0 \in L^2$.

Thus this equation is an excellent candidate to iterative solution. We will see in the following how we can solve such equation using the conjugate gradient iterative method.

2.2. The Modified CGM Formulation

The conjugate gradient method is proposed as an alternative algorithm for treating ill-conditioned systems, since, there is no rounding errors building from one iteration step to the other [8]. Also, after each iteration the quality of the solution is known in the conjugate gradient method.

The method proceeds by generating successive approximations to the solution, and search directions used in updating iterates and residuals. Only a small number of vectors need to be kept in memory. Also the solution is improved at a steady rate throughout the iterative process.

The first step in the computation process is evaluation of the term $\hat{Z}J$. Some transformations are needed in order to compute this term.

The impedance operator used here is described using modal basis, it is a discrete operator applied on the spectral domain. It is also called a spatial-spectral operator and it allows transition from spectral to spatial domain

If we apply the impedance operator on J we obtain:

$$\widehat{Z}J = \sum_n |f_n\rangle z_n \langle f_n \,|\, J\rangle \tag{9}$$

The unknown function J is approximated by a linear combination of N independent pulse function [3] $\{g_i(x)\}$ with N unknowns coefficients $J_1, J_2, \ldots, J_N$:

$$J(x) = \sum_{i=1}^{N} J_i g_i(x) \tag{10}$$

Since the x-axis is divided into N equivalent segments with negligible width and the current is assumed to be constant over each segment, the hermitian scalar product can be approximated by

$$< f_n(x)| \, J(x) > = \sum_i f_n(x_i) J(x_i) \Delta x_i \tag{11}$$

Δx_i is the uniform distance between any two sampling point x_i and x_{i+1}, it is equal to a/N and is called the cell density. We will note it Δ in the subsequent parts of this paper.

The operator equation can then be written in the discrete domain as follows:

$$\widehat{Z}J(x) = \sum_n \left(\sum_i f_n(x_i)J(x_i)\Delta \right) z_n f_n(x) \tag{12}$$

The equation to solve, using the CG method is then given by:

$$\sum_n \left(\sum_i f_n(x_i)J(x_i)\Delta \right) z_n f_n(x) = -E_0 \tag{13}$$

The algorithm starts with an initial guess J of the unknown current. In all cases examined here a zero estimate is used. The initial residual and direction vectors are computed as following:

$$r_0 = \widehat{\mathrm{H}}_{\mathrm{m}} E_0$$
$$p_0 = r_0 \tag{14}$$

We remind that $\widehat{\mathrm{H}}_{\mathrm{m}}$ is the indicator of the metallic part of the discontinuity surface $\begin{array}{l} \widehat{\mathrm{H}}_{\mathrm{m}} = 1 \ on \ the \ metal \\ \widehat{\mathrm{H}}_{\mathrm{m}} = 0 \ on \ the \ dielectric \end{array}$.

Among the algorithm steps we remind the compute of the following terms at the kth iteration:

$$w_k = \widehat{\mathrm{H}}_{\mathrm{m}}\widehat{Z}p_k \tag{15}$$

$$\alpha_k = \frac{\|r_k\|^2}{p_k^T w_k} \tag{16}$$

$$J_{k+1} = J_k + \alpha_k p_k \tag{17}$$

where p_k is the direction vector and α_k is the scalar coefficient [5, 6].

The values of the current obtained at the kth iteration are stored in the column vector J_k, with N components. Hence the ith element of J for example is the initial guess for the current over the ith segment.

We achieve then, all the algorithm steps [5, 6].

The stopping test used to decide about the convergence of the CG algorithm is the normalized squared residual error expressed as follow:

$$Err_k = \frac{\|r_k\|}{\|E_0\|} < \varepsilon \tag{18}$$

where ε is the accuracy fixed.

Experimental results obtained using the new formulation of the CG method are detailed in the subsequent section.

3. NUMERICAL RESULTS

3.1. Case of an Iris

Let us consider the structure given in Figure 1(a) consisting of an iris located in the cross section of a rectangular waveguide. The CG algorithm is then implemented in order to determine the current J. We follow the different algorithm steps exposed on the previous section.

We have two types of convergence, one is related to the error criterion and the second is attached to the mode convergence. In fact, the iteration process is continued till $Err_k = \frac{\|r_k\|}{\|E_0\|} < \varepsilon$. In this work, we assume that the CG algorithm converges when $\varepsilon = 0.001$.

Figure 3 shows the convergence of the CGM for the iris structure, in an EMEM waveguide and in an electric waveguide, all with the cell density fixed at a/200.

It is observed that the rate of convergence of the CGM is independent upon the waveguide. In fact, the residual error has the same behavior for the two types of waveguides.

The CG method adopted requires at about 8 iterations to reduce the residual norm below 0.001 with a cell density of a/200.

We represent on the following, the current density behavior as a function of the iterations number and the mode number.
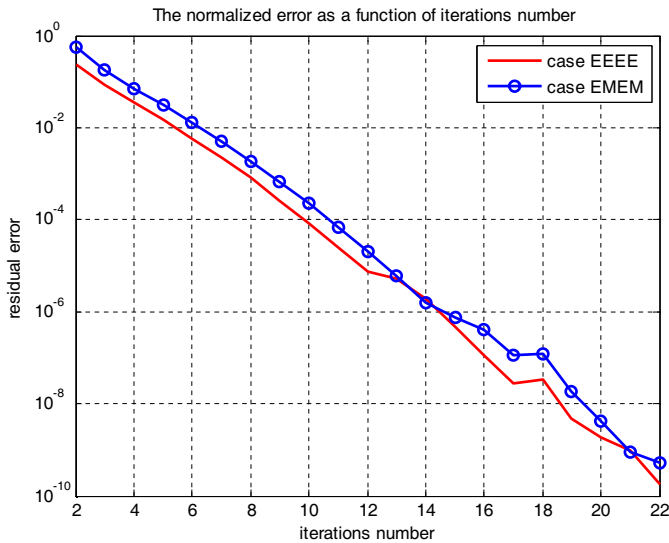

Figure 3. Convergence of the CGM for iris structures in the case of EMEM and EEEE waveguides ($a = 22.9\,\text{mm}$, $F = 9\,\text{GHz}$, $N = 200$, $n = 4000$).
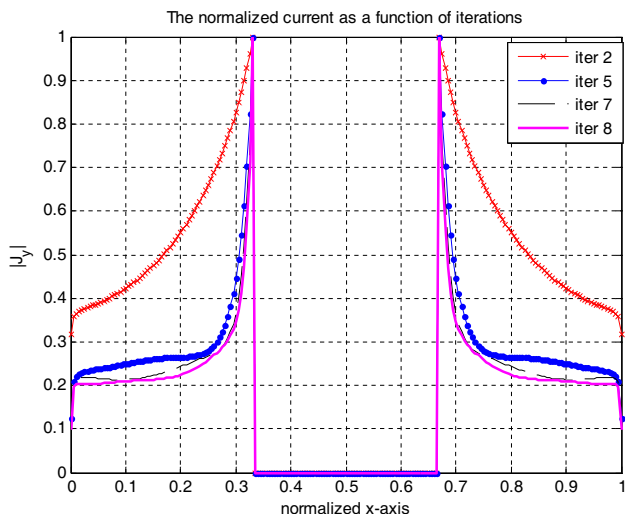
Figure 4. Numerical convergence of the normalized current distribution evaluated by the CG method as a function of iterations number (case of an EMEM waveguide); $a = 10\,\text{mm}$, $d = a/3$, $F = 2\,\text{GHz}$, $N = 200$.
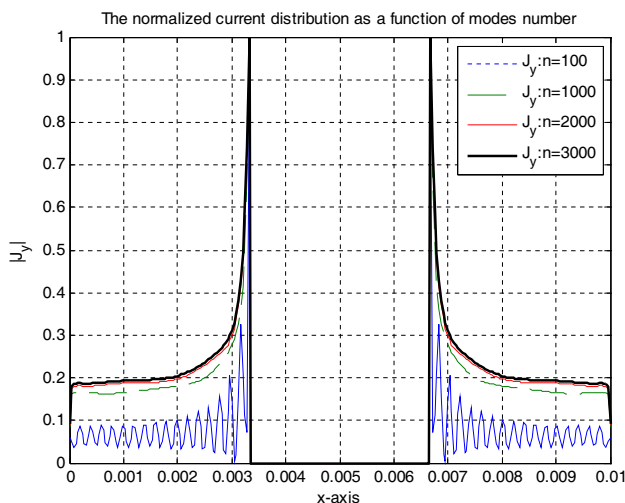

Figure 5. Numerical convergence of the normalized current distribution evaluated by the CG method as a function of modes number; (case of an EMEM waveguide); $a = 10\,\text{mm}$, $d = a/3$, $F = 2\,\text{GHz}$, $N = 200$.

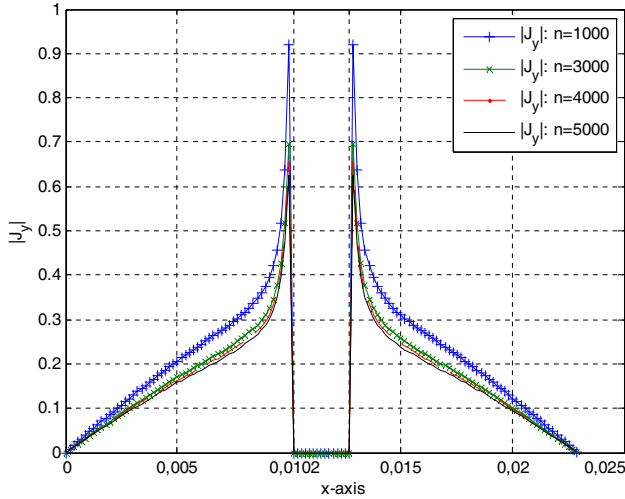**Figure 6.** The current distribution for an irregular inductive iris as a function of the mode number (case of an EEEE guide); $a = 22.9\,\text{mm}$, $d = a/9$, $N = 128$, $F = 9\,\text{GHz}$.

Figure 4 shows that the current evaluated by the CG and obtained at convergence is conform to theory with respect to the boundary conditions.

Figure 5 represents the current behavior as a function of the mode number. It shows that the mode convergence is obtained for $n = 3000$.

We have also tested the current distribution over the iris structure, for an electric guide. Result obtained is drawn in Figure 6.

It is observed that for a case of electric waveguide the mode convergence is obtained for $n = 4000$. Also result obtained is conforming to theory with respect to the boundary conditions.

3.2. Case of a Post

Let's consider the structure given in Figure 1(b) consisting of a post located in the cross section of a rectangular waveguide. We apply the modified CG algorithm adopted in this work in order to determine the current distribution.

Figure 7 shows the convergence rates of the two examples of posts respectively in an EMEM waveguide and in an electric waveguide with cell density of a/200.

It is observed that the method converges to a good solution at about 6 iterations, even thought the initial guess was taken to be zero.
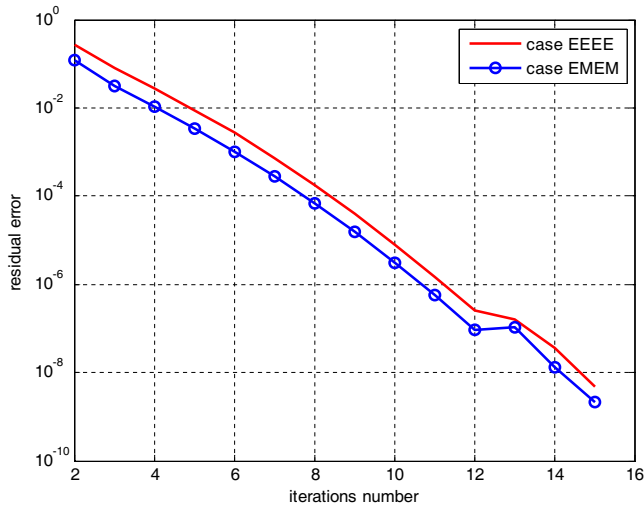
Figure 7. Convergence of the CGM for post structures in the case of EMEM and EEEE waveguides ($a = 22.9\,\text{mm}$, $F = 9\,\text{GHz}$, $N = 200$, $n = 4000$).

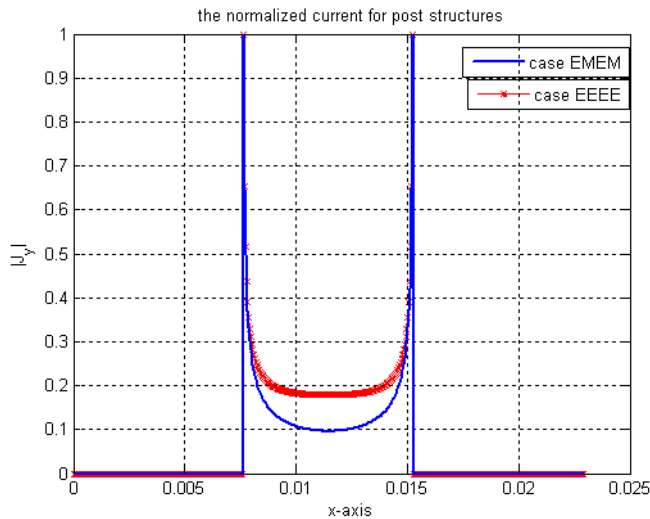**Figure 8.** The current distribution evaluated by the CG method for a post located on the cross section of EMEM and EEEE waveguides; $a = 22.9\,\text{mm}$, $d = a/3$, $F = 9\,\text{GHz}$, $N = 500$, $n = 4000$.

Note that the rate of convergence in these examples is faster than in the previous examples shown in Figure 3. In fact, in this case, the metallic surface is smaller than the one used for iris structure, and the current is assumed to be null on the major part of the structure, which exhibit less operations for the algorithm.

Figure 8 shows the current distribution for post structures respectively in an EMEM waveguide and in an electric guide.

The obtained results are conforming to theory with respect to boundary conditions. It is also observed that, the waveguide walls have an influence on the current distribution. In fact, for the same cell density, the current has the same behavior but not the same numerical intensity for the two kinds of waveguides. This is related to the difference on the excitation modes used for the two kinds of waveguides.

4. VALIDATION OF THE NEW CGM IMPLEMENTATION

4.1. CGM Versus MoM

After one obtains the induced electric current J_y numerically over the metallic surface, with a given excitation E, other parameters, such as the scattered and the total electric fields can be easily deduced.

In this section, the total electric field is determined and compared to the one found by the MoM.

The electric field is computed by:

$$E = E_0 + \widehat{Z}J \tag{19}$$

Figure 9 draws the normalized total electric field evaluated by the conjugate gradient method and the one computed by the moment method (Galerkin method) for the iris structure with EMEM walls.

For the moment method, results are plotted for 4000 sinusoidal mode functions; the test functions used are 200.

Figure 9 shows that the electric field behavior is with respect to the boundary conditions It is also observed that result found at convergence by the CGM is conforming to the ones found by the MoM.

Let's remind that the CG method on which we are based in this work, exhibit less storage comparing to the MoM, it has also less numerical complexity, which make it more convenient. In fact, with the CGM, there is no need to stock nor to inverse a matrix. The complexity of this method is $O(N^2)$, and the storage is $O(N)$. Also, convergence is guaranteed after a small number of iterations.
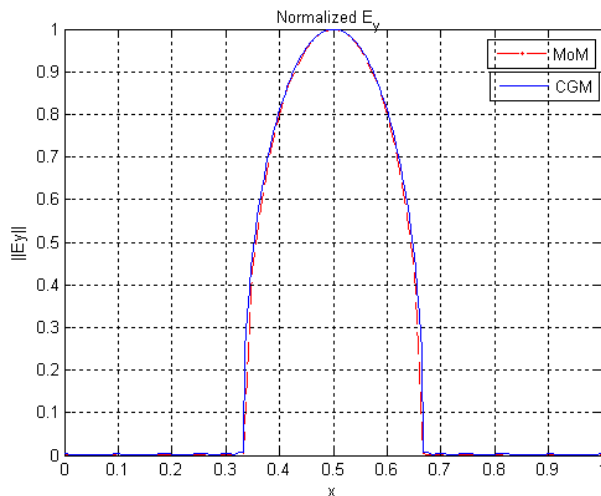
Figure 9. The normalized electric field depicted by the CGM adopted in this work and the one evaluated by the traditional Galerkin method, with $a = 10\,\text{mm}$, $b = 5\,\text{mm}$, $d = a/3$ at $F = 2\,\text{GHz}$ (case of an EMEM guide). MoM: $f_n = 3000$, $g_p = 200$; CGM: $f_n = 3000$, $N = 200$.

4.2. Analytical Validation of the Method

As a further test on the validity of this method, results obtained have been compared with Marcuvitz's formulae [17]. The input impedance parameter has been computed by the CG method adopted in this work and has been compared to the one analytically computed by Markuvitz.

The input impedance is computed as following

$$Z_{in} = \frac{< E_0, E_0 >}{2 < E_0, J >} \tag{20}$$

The $1/2$ factor translated the contribution of the two half spaces on both sides of the discontinuity.

E_0 designs the excitation of an EEEE waveguide, and J is the current determined at convergence by the CG algorithm adopted in this work.

Figure 10 depicts the convergence of the input impedance parameter as a function of frequency.

It is observed that the input impedance obtained using the CG method, presented in this paper, is considerably approached to the one computed by Markuvitz especially in the low frequency band. In its book, Markuvitz is computing Z_{in} analytically using the equivalent
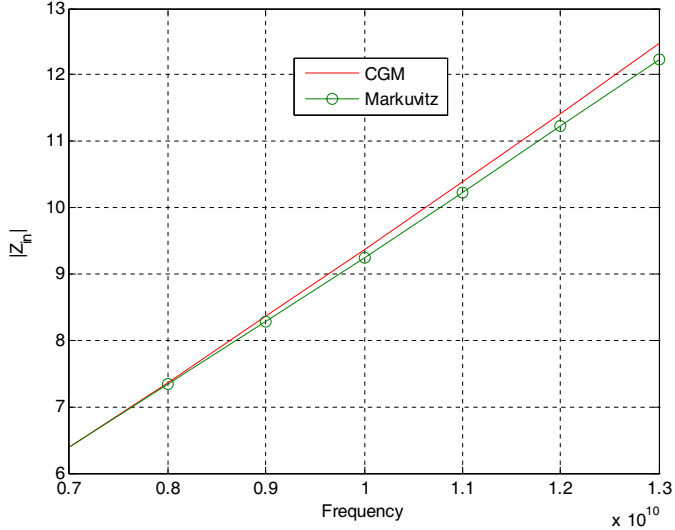
Figure 10. Zin-parameter as a function of frequency for the inductive iris structure in an EEEE waveguide. Dimensions are: $a = 22.9\,\text{mm}$, $d = a/9$, $n = 4000$, $N = 500$.

static method and the lowest mode, in our case; we are using a complete basis mode.

5. CONCLUSION

A new formulation of the CG method was presented in this paper to solve electromagnetic scattering problem. The conventional CG algorithm was combined to the generalized equivalent circuit method to get an original formulation. This technique is based on the impedance operator and is applied to structures with discontinuities on a rectangular waveguide The obtained equation was expressed as a function of the impedance operator which is a spatial-spectral operator allowing an easy transition from spectral to spatial domain. This method exhibits O(N) memory storage and O(N^2) addition/multiplication operations.

This method converges to the solution in a finite small number of steps starting from a zero initial guess. Some numerical examples are given to illustrate the properties of this method.

The current and the electric field behaviors have been determined using this method. For validation purposes, the computed results were compared to those obtained by the MoM and the analytical results of

Markuvitz.

The primary area of future work is to validate this method for more complicated structures.

REFERENCES

1. Tsang, L., J. A. Kong, and K. Ding, *Scattering of Electromagnetic Waves: Theories and Applications*, John Wiley and Sons, Canada, 2000.

2. Fleming, A. H. J., "A finite element method for composite scatterers," *Progress In Electromagnetic Research*, Vol. 2, 69–112, 1990.

3. Harrington, R. F., *Field Computation by Moment Methods*, Macmillan, New York, 1968

4. Harrington, R. F. and T. K. Sarkar, "Boundary elements and the method of moments," *5th Int. Conf. Boundary Elements*, 31–40, Hiroshima, Japan, November 8–11, 1983.

5. Nocedal, J. and S. Wright, *Numerical Optimization, Springer Series in Operations Research*, Springer-Verlag, New York, 1999.

6. Sarkar, T. K., "The conjugate gradient method as applied to electromagnetic field problems," *IEEE Antennas and Propagation Society Newsletter*, August 1986.

7. Volakis, J. L. and K. Barkeshli, "Applications of the conjugate gradient FFT method to radiation and scattering," *Progress In Electromagnetic Research*, Vol. 5, 159–239, 1991.

8. Peterson, A. F., S. L. Ray, C. H. Chan, and R. Mittra, "Numerical implementation of the conjugate gradient method and the Cg-FFT for electromagnetic scattering," *Progress In Electromagnetic Research*, Vol. 5, 241–300, 1991.

9. Sarkar, T. K., E. Arvas, and S. M. Rao, "Application of FFT and the conjugate gradient method for the solution of electromagnetic radiation from electrically large and small conducting bodies," *IEEE Trans. Antennas Propagat.*, Vol. 34, No. 5, 635–640, 1986.

10. Peterson, A. F. and R. Mittra, "Convergence of the conjugate gradient method when applied to matrix equations representing electromagnetic scattering problems," *IEEE Trans. Antennas Propagat.*, Vol. 34, 1447–1454, 1986.

11. Barkeshli, K. and J. L. Volakis, "Improving the convergence rate of the conjugate gradient FFT using subdomain basis functions," *IEEE Trans. Antennas Propagat.*, Vol. 37, No. 7, 893–900, 1989.

12. Cwik, T. A. and R. Mittra, "Scattering from a periodic array of

free-standing arbitrarily shaped perfectly conducting or resistive patches," *IEEE Trans. Antennas Propagat.*, Vol. 35, 1226–1234, 1987.

13. Baudrand, H., "Representation by equivalent circuit of the integrals methods in microwave passive elements," *European Microwave Conference*, Vol. 2, 1359–1364, Budapest, Hungary, September 10–13, 1990.

14. Aguili, T., "Modélisation des composantes SFH planaires par la méthode des circuits équivalents généralisés," Thesis Manuscript, National Engineering School of Tunis, Tunisia, 2000.

15. Baudrand, H. and D. Bajon, "Equivalent circuit representation for integral formulations of electromagnetic problems," *International Journal of Numerical Modelling-electronic Networks Devices and Fields*, Vol. 15, 23–57, January–February 2002.

16. Aubert, H. and H. Baudrand, *L'Electromagnétisme par les Schémas Equivalents*, Cepaduès Éditions, 2003.

17. Markuwitz, N., *Waveguide Handbook*, Wiley-Interscience, New York, 1986.

18. Collin, E. R., *Foundations for Microwave Engineering*, Donald G. Dudley, Series Editor, IEEE Press, 2001.

19. Baudrand, H., *Introduction au Calcul des Eléments de Circuits Passifs en Hyperfréquence*, Cepaduès Éditions, 2001.